symmetry

MDPI

Article

Dynamics of Shunting Inhibitory Cellular Neural Networks with Variable Two-Component Passive Decay Rates and Poisson Stable Inputs

Marat Akhmet [1,*], Madina Tleubergenova [2,3] and Akylbek Zhamanshin [1,2]

1 Department of Mathematics, Middle East Technical University, Ankara 06531, Turkey; akylbek78@mail.ru
2 Department of Mathematics, Aktobe Regional University, Aktobe 030000, Kazakhstan; madina_1970@mail.ru
3 Institute of Information and Computational Technologies CS MES RK, Almaty 050010, Kazakhstan
* Correspondence: marat@metu.edu.tr; Tel.: +90-312-210-53-55

Abstract: Shunting inhibitory cellular neural networks with continuous time-varying rates and inputs are the focus of this research. A new model is considered with compartmental passive decay rates which consist of periodic and Poisson stable components. The first component guarantees the Poisson stability of the dynamics, and the second one causes irregular oscillations. The inputs are Poisson stable to take into account the more sophisticated environment of the networks. The rates and inputs are synchronized to obtain Poisson stable outputs. A new efficient technique for checking the recurrence, the method of included intervals, is applied. Sufficient conditions for the existence of a Poisson stable solution and its asymptotic stability were obtained. Numerical simulations of Poisson stable outputs as well as inputs are provided. Examples of the model with Poisson stable rates, inputs and outputs confirm the feasibility of theoretical results. Discussions were undertaken to provide additional light on the relation of the obtained results with practical and theoretical potentials of neuroscience. Quantitative characteristics are suggested, which can be useful for the future applications of the results. In particular, the center of antisymmetry for the degree of periodicity is determined.

Keywords: shunting inhibitory cellular neural networks; compartmental passive decay rate; Poisson stable inputs, outputs and rates; the method of included intervals; asymptotic stability of outputs

Citation: Akhmet, M.; Tleubergenova, M.; Zhamanshin, A. Dynamics of Shunting Inhibitory Cellular Neural Networks with Variable Two-Component Passive Decay Rates and Poisson Stable Inputs. *Symmetry* **2022**, *14*, 1162. https://doi.org/10.3390/sym14061162

Academic Editor: Sergio Elaskar

Received: 10 May 2022
Accepted: 1 June 2022
Published: 5 June 2022

1. Introduction

Cellular neural networks (CNNs), introduced in [1], immediately gained wide recognition to focus on parallel asynchronous computing processes. In recent years, many algorithms for image processing, pattern recognition, evaluation of the dynamics of mechanical systems, etc., were successfully implemented with CNNs.

Shunting inhibitory cellular neural networks (SICNNs) were proposed in [2] and have been extensively applied in psychophysics, optimization, speech, robotics, adaptive pattern recognition, vision and image processing, among other tasks.

In SICNNs, neighboring cells exert mutual inhibitory interactions of the shunting type. In its original formulation, they describe the dynamics of the cell C_{ij}, $i = 1, \dots, m$, $j = 1, \dots, n$, by the following nonlinear ordinary differential equation,

$$x'_{ij}(t) = -a_{ij}x_{ij}(t) - \sum_{C_{kl} \in N_r(i,j)} C_{ij}^{kl} f(x_{kl}(t))x_{ij}(t) + v_{ij}(t). \quad (1)$$

Here, x_{ij} indicates the ijth neuron state, coefficient a_{ij} represents the passive decay rate, $C_{ij}^{kl} \geq 0$ denotes the strength of the coupling of the cell C_{kl} conveyed to the cell C_{ij}, $f(x_{kl})$ is the activation function, and $v_{ij}(t)$ is the external input to cell C_{ij}.

SICNNs are a grid of cells, such that each cell C_{ij} is connected with cells of its r-neighborhood. Here, we follow the definition in [1], where the r-neighborhood $N_r(i,j)$ is defined as

$$N_r(i,j) = \{C_{kl} : \max(|k-i|, |l-j|) \leq r,\ 1 \leq k \leq m, 1 \leq l \leq n\},$$

with fixed natural numbers m and n.

It is of strong interest to replace the constant rates in SICNNs by time-varying ones, and many researchers have investigated the dynamic behavior of SICNNs, wherein passive decay rates are periodic [3], anti-periodic [4,5], almost periodic [6–8] and pseudo-periodic [9,10] functions.

We investigate the following SICNNs with continuous time-varying coefficients:

$$x'_{ij}(t) = -(a_{ij}(t) + b_{ij}(t))x_{ij}(t) - \sum_{C_{kl} \in N_r(i,j)} C_{ij}^{kl} f(x_{kl}(t))x_{ij}(t) + v_{ij}(t), \tag{2}$$

where the rates are compartmental and consist of two components such that $a_{ij}(t)$ are periodic whilst $b_{ij}(t)$ and inputs $v_{ij}(t)$ are Poisson stable functions.

The following concept is fundamental for the present study.

Definition 1 ([11])**.** *A function $\psi(t)$: $\mathbb{R} \to \mathbb{R}$, bounded and continuous, is said to be Poisson stable if there is a sequence of moments t_p, $t_p \to \infty$ as $p \to \infty$, such that the uniform convergence $\psi(t + t_p) \rightrightarrows \psi(t)$ is valid on each bounded interval of the real axis.*

Consider the sequence τ_p, $p = 1, 2, \dots$, such that $t_p = \tau_p(mod\omega)$, and $\omega > 0$ is a fixed number. It is clear that $0 \leq \tau_p < \omega$. Hence, there exists a subsequence τ_{p_l}, $l = 1, 2, \dots$, which converges to a real number τ_ω. Consequently, one can find a subsequence t_{p_l}, $l = 1, 2, \dots$, of the *convergence sequence* t_p, such that $t_{p_l} \to \tau_\omega (mod\ \omega)$ as $l \to \infty$. The number τ_ω is said to be *Poisson shift* for the convergence sequence. The set of all Poisson shifts, $\mathcal{T}_\omega$, is not empty, and is of several or even infinite number elements. In what follows, $\kappa_\omega = inf\ \mathcal{T}_\omega$, $0 \leq \kappa_\omega < \omega$, is called *the Poisson number* for t_p, $p = 1, 2, \dots$, and ω.

2. Methods

It is historical fact that Poisson stability emerged in works [12,13] and then spread to many areas of applied mathematics, similarly to how periodic, quasi-periodic and almost periodic motions [14–19] spread. In recent decades, the dynamics were intensively considered in neuroscience [3,6–8,20–24]. Currently, Poisson stable motions are the most sophisticated type of recurrence [25–28].

It is natural to assume that Poisson stable motions should be considered in neuroscience due to the arguments common with those for other types of recurrence, such as periodicity and almost periodicity. The dynamics admit an additional significant reason to be involved in research since it is strongly adjoint with chaos [29].

A new technique, *the method of included intervals*, was introduced and developed in papers [30–35] and book [36] to approve Poisson stability for solutions in differential equations and neural networks. The approach strongly differs from the comparability method in [37–40].

In papers [33–35], it is shown that the Poisson stable motions became chaotic if one equipped them with the unpredictability property. It is a very remarkable result since it was proven that a chaotic trajectory can be Poisson stable and vice versa. Moreover, the dynamics are enriched with infinitely many unstable recurrent motions [36,41,42] which strongly relate to the cognitive activity [43–46]. This is why one can apply to the dynamics of neural networks effective methods of chaos control such as OGY method and Piragas method, which are very useful in neural models study and their applications [47].

In this paper, SICNNs with Poisson stable passive decay rates and inputs are studied. Moreover, the rates of cell activity have a special structure consisting of two components.

One of them is periodic, responsible for the overall dynamics and stability whilst the second is Poisson stable, causing irregular behavior in SICNNs. The passive decay rates and inputs are synchronized by the common moments of convergence on bounded intervals. The relationship between periodic and Poisson stable functions has been studied in [32].

3. Main Results

Using the result for differential equations [48], one can convince that the following lemma is valid.

Lemma 1. *A function $y(t) = (y_{ij}(t))$, $i = 1,\ldots,m$, $j = 1,\ldots,n$, bounded on the real axis, is a solution of (2) if and only if the following equations are true,*

$$y_{ij}(t) = -\int_{-\infty}^{t} e^{-\int_s^t a_{ij}(u)du}\Big(b_{ij}(s)y_{ij}(s) + \sum_{C_{kl}\in N_r(i,j)} C_{ij}^{kl} f(y_{kl}(s))y_{ij}(s) - v_{ij}(s)\Big)ds. \tag{3}$$

Throughout the paper, the norm for bounded functions $u : \mathbb{R} \to \mathbb{R}$, $\|u\| = \sup_{t\in\mathbb{R}} |u(t)|$, will be used.

Denote by $\mathcal{B}$ the set of rectangle matrix-functions $\phi(t) = (\phi_{ij}(t))$, $i = 1,2,\ldots,m$, $j = 1,2,\ldots,n$, with Poisson stable entries such that $|\phi_{ij}(t)| < H$, $i = 1,2,\ldots,m$, $j = 1,2,\ldots,n$, where H is a positive number. All the functions are with the common convergence sequence t_p, $p = 1,2,\ldots$. Moreover, determine the norm $\|\phi(t)\|_0 = \max_{i,j} \|\phi_{ij}(t)\|$ in the set.

Let us define the operator $\Pi\phi(t) = (\Pi_{ij}\phi(t))$, $\phi \in \mathcal{B}$, $i = 1,\ldots,m$, $j = 1,\ldots,n$, where

$$\Pi_{ij}\phi(t) \equiv -\int_{-\infty}^{t} e^{-\int_s^t a_{ij}(u)du}\Big(b_{ij}(s)\phi_{ij}(s) + \sum_{C_{kl}\in N_r(i,j)} C_{ij}^{kl} f(\phi_{kl}(s))\phi_{ij}(s) - v_{ij}(s)\Big)ds. \tag{4}$$

We shall need the following assumptions:

(C1) The functions $a_{ij}(t)$ are ω-periodic, such that $\int_0^\omega a_{ij}(u)du > 0$, $i = 1,\ldots,m$, $j = 1,\ldots,n$;

(C2) Functions $b_{ij}(t)$ and $v_{ij}(t)$, $i = 1,2,\ldots,m$, $j = 1,2,\ldots,n$, are Poisson stable with the common convergence sequence t_p, $p = 1,2,\ldots$;

(C3) The Poisson number κ_ω is equal to zero;

(C4) $\exists\, m_f > 0$ such that $\sup_{|s|<H} |f(s)| = m_f$;

(C5) $\exists\, L > 0$ such that $|f(s_1) - f(s_2)| \le L|s_1 - s_2|$ if $|s_1| < H, |s_2| < H$.

Condition $(C1)$ implies that there exist constants $K_{ij} \ge 1$, $\lambda_{ij} > 0$ which satisfy

$$e^{-\int_t^s a_{ij}(u)du} \le K_{ij}e^{-\lambda_{ij}(t-s)},$$

for all $i = 1,\ldots,m$, $j = 1,\ldots,n$.

We will use notations:

$$m_{ij}^b = \sup_{t\in\mathbb{R}} |b_{ij}(t)|, \quad m_{ij}^v = \sup_{t\in\mathbb{R}} |v_{ij}(t)|, i = 1,2,\ldots,m, j = 1,2,\ldots,n.$$

The additional assumptions are required.

(C6) $K_{ij}(m_{ij}^b + (m_f + LH)\sum_{C_{kl}\in N_r(i,j)} C_{ij}^{kl}) < \lambda_{ij}$, $i = 1,\ldots,m$, $j = 1,\ldots,n$;

(C7) $\dfrac{K_{ij}m_{ij}^v}{\lambda_{ij} - K_{ij}m_f\sum_{C_{kl}\in N_r(i,j)} C_{ij}^{kl} - K_{ij}m_{ij}^b} < H$, $i = 1,\ldots,m$, $j = 1,\ldots,n$.

Lemmas A1 and A2 for the following proof are from Appendix A.

Theorem 1. *Suppose that assumptions (C1)–(C7) hold; then, the system (1) admits a unique asymptotically stable Poisson stable solution.*

Proof. Firstly, we prove the completeness of $\mathcal{B}$. Let $\phi^k(t) = (\phi^k_{ij}(t))$, $i = 1,2,\ldots,m$, $j = 1,2,\ldots,n$, be a sequence converging on $\mathbb{R}$ to a limit function $\phi(t)$. Consider a section $[a,b]$, $-\infty < a < b < \infty$, and $i = 1,2,\ldots,m, j = 1,2,\ldots,n$. We have that

$$|\phi_{ij}(t+t_p) - \phi_{ij}(t)| \leq |\phi_{ij}(t+t_p) - \phi^k_{ij}(t+t_p)| + |\phi^k_{ij}(t+t_p) - \phi^k_{ij}(t)| + |\phi^k_{ij}(t) - \phi_{ij}(t)|. \tag{5}$$

For sufficiently large p and k, it can be attained that each term on the right hand-side of (5) is less than $\frac{\epsilon}{3}$ for an arbitrary small $\epsilon > 0$ and $t \in [a,b]$. The inequalities $|\phi_{ij}(t+t_p) - \phi_{ij}(t)| < \epsilon$, $i = 1,2,\ldots,m, j = 1,2,\ldots,n$, imply that $\phi(t+t_p) \to \phi(t)$ uniformly on $[a,b]$. The completeness of $\mathcal{B}$ is shown.

Under conditions (C1)–(C7), the operator Π is invariant in $\mathcal{B}$ (see Lemma A1) and contractive (see Lemma A2). According to the contraction mapping theorem, there exists a unique Poisson stable solution, $z(t) = (z_{ij}(t))$, $i = 1,2,\ldots,m, j = 1,2,\ldots,n$, of the neural network (2).

Now, consider the stability of solution $z(t)$. It is correct that for all $i = 1,\ldots,m$, $j = 1,\ldots,n$,

$$z_{ij}(t) = e^{-\int_{t_0}^t a_{ij}(u)du} z_{ij}(t_0) - \int_{t_0}^t e^{-\int_s^t a_{ij}(u)du}\Big(b_{ij}(s)z_{ij}(s) + \sum_{C_{kl}\in N_r(i,j)} C^{kl}_{ij} f(z_{kl}(s))z_{ij}(s) - v_{ij(s)}\Big)ds.$$

Let $x(t) = (x_{ij}(t))$, $i = 1,\ldots,m, j = 1,\ldots,n$, be another solution of model (2). One can write that

$$x_{ij}(t) = e^{-\int_{t_0}^t a_{ij}(u)du} x_{ij}(t_0) - \int_{t_0}^t e^{-\int_s^t a_{ij}(u)du}\Big(b_{ij}(s)x_{ij}(s) + \sum_{C_{kl}\in N_r(i,j)} C^{kl}_{ij} f(x_{kl}(s))x_{ij}(s) - v_{ij(s)}\Big)ds.$$

Using the formula

$$\begin{aligned}
&x_{ij}(t) - z_{ij}(t) = e^{-\int_{t_0}^t a_{ij}(u)du}(x_{ij}(t_0) - z_{ij}(t_0)) - \int_{t_0}^t e^{-\int_{t_0}^t a_{ij}(u)du}\Big(b_{ij}(s)x_{ij}(s) - b_{ij}(s)z_{ij}(s) + \\
&\sum_{C_{kl}\in N_r(i,j)} C^{kl}_{ij} f(x_{kl}(s))x_{ij}(s) - \sum_{C_{kl}\in N_r(i,j)} C^{kl}_{ij} f(z_{kl}(s))z_{ij}(s)\Big)ds = e^{-\int_{t_0}^t a_{ij}(u)du}(x_{ij}(t_0) - z_{ij}(t_0)) - \\
&\int_{t_0}^t e^{-\int_{t_0}^t a_{ij}(u)du}\Big(b_{ij}(s)x_{ij}(s) - b_{ij}(s)z_{ij}(s) + \sum_{C_{kl}\in N_r(i,j)} C^{kl}_{ij} f(x_{kl}(s))x_{ij}(s) - \\
&\sum_{C_{kl}\in N_r(i,j)} C^{kl}_{ij} f(z_{kl}(s))x_{ij}(s) + \sum_{C_{kl}\in N_r(i,j)} C^{kl}_{ij} f(z_{kl}(s))x_{ij}(s) - \sum_{C_{kl}\in N_r(i,j)} C^{kl}_{ij} f(z_{kl}(s))z_{ij}(s)\Big)ds,
\end{aligned}$$

we have that

$$\begin{aligned}
&|x_{ij}(t) - z_{ij}(t)| \leq e^{-\int_{t_0}^t a_{ij}(u)du}|x_{ij}(t_0) - z_{ij}(t_0)| + \int_{t_0}^t e^{-\int_{t_0}^t a_{ij}(u)du}\Big(|b_{ij}(s)||x_{ij}(s) - z_{ij}(s)| + \\
&\sum_{C_{kl}\in N_r(i,j)} C^{kl}_{ij}|f(x_{kl}(s)) - f(z_{kl}(s))||x_{ij}(s)|ds + \sum_{C_{kl}\in N_r(i,j)} C^{kl}_{ij}|f(z_{kl}(s))||x_{ij}(s) - z_{ij}(s)|\Big)ds \leq \\
&K_{ij}e^{-\lambda_{ij}(t-t_0)}|x_{ij}(t_0) - z_{ij}(t_0)| + \int_{t_0}^t K_{ij}e^{-\lambda_{ij}(t-t_0)}\Big(m^b_{ij} + (LH + m_f)\sum_{C_{kl}\in N_r(i,j)} C^{kl}_{ij}\Big)|x_{ij}(s) - z_{ij}(s)|ds,
\end{aligned}$$

for all $i = 1,2,\ldots,m, j = 1,2,\ldots,n$.

Apply the Gronwall–Bellman Lemma to get

$$|x_{ij}(t) - z_{ij}(t)| \leq K_{ij}|x_{ij}(t_0) - z_{ij}(t_0)|e^{(K_{ij}(m^b_{ij} + (m_f + LH)\sum_{C_{kl}\in N_r(i,j)} C^{kl}_{ij}) - \lambda_{ij})(t-t_0)},$$

for each $i = 1,2,\ldots,m, j = 1,2,\ldots,n$.

The condition (C6) confirms that the solution $z(t)$ is asymptotically stable. □

We shall then illustrate the theoretical results by numerical simulations.

It is known [49] that there exists a Poisson stable sequence ρ_i, $i \in \mathbb{Z}$, which is the solution for the logistic discrete equation

$$\lambda_{i+1} = \mu\lambda_i(1-\lambda_i), \tag{6}$$

where $i \in \mathbb{Z}$, and $\mu \in [3+(2/3)^{1/2}, 4]$ is a fixed parameter. The sequence is a discrete version of the Poisson stable function. The section $[0,1]$ is invariant with respect to (6) for the considered values of μ.

In the examples below, we will use the Poisson stable function $\Theta(t)$ [49] which is the unique bounded on the real axis solution of differential equation

$$\Theta' = -3\Theta + W(t), \tag{7}$$

where $W(t) = \rho_i$ for $t \in [hi, h(i+1)), i \in \mathbb{Z}$ and h is a positive real number. The number h is called *the length of step* for the piecewise constant function $W(t)$, and for the function $\Theta(t)$.

Example 1. *Let us consider the system,*

$$\frac{dx_{ij}}{dt} = -(a_{ij}(t) + b_{ij}(t))x_{ij} - \sum_{C_{kl}\in N_1(i,j)} C_{ij}^{kl} f(x_{kl})x_{ij} + v_{ij}(t), \tag{8}$$

where $i = 1,2$, $j = 1,2,3$, $f(s) = 0.5arctan(s)$, $C_{ij}^{11} = 0.04$, $C_{ij}^{12} = 0.03$, $C_{ij}^{13} = 0.05$, $C_{ij}^{21} = 0.01$, $C_{ij}^{22} = 0.06$, $C_{ij}^{23} = 0.02$. For each fixed $k = 1,2$, and $l = 1,2,3$, the coefficients C_{ij}^{kl} are the same for all i,j, such that the cell C_{kl} belongs to $N_1(i,j)$. The functions $a_{ij}(t)$ are periodic with period $\omega = \pi$, such that $a_{11}(t) = 3+\cos(4t)$, $a_{12}(t) = 2+\sin(2t)$, $a_{13}(t) = 4+\sin(4t)$, $a_{21}(t) = 5+\cos(2t)$, $a_{22}(t) = 3+\sin(6t)$, $a_{23}(t) = 6+\sin(4t)$. The functions $b_{ij}(t)$ and $v_{ij}(t)$ are Poisson stable, $b_{11}(t) = 0.5\Theta(t)$, $b_{12}(t) = 0.3\Theta(t)$, $b_{13}(t) = 0.2\Theta(t)$, $b_{21}(t) = 0.7\Theta(t)$, $b_{22}(t) = 0.8\Theta(t)$, $b_{23}(t) = 0.3\Theta(t)$, $v_{11}(t) = 5\Theta(t)$, $v_{12}(t) = 4\Theta^2(t)$, $v_{13}(t) = -\Theta(t)$, $v_{21}(t) = 2\Theta(t)$, $v_{22}(t) = 7\Theta^3(t)$, $v_{23}(t) = 2\Theta^2(t)$, where $\Theta(t)$ is the solution of Equation (7) with the step of length $h = 3\pi$. Below, we shall need the degree of periodicity, $\kappa = \omega/h$, which in the present case is equal to $1/3$.

Since the elements of the convergence sequence t_i, $i \in \mathbb{Z}$ are multiples of h and the period ω is equal to the Poisson number π, κ_ω is equal to zero. Furthermore, $\sup_{t\in\mathbb{R}} |b_{ij}(t)| = m_{ij}^b$, $\sup_{t\in\mathbb{R}} |v_{ij}(t)| = m_{ij}^v$, where $m_{11}^b = 0.17, m_{12}^b = 0.1, m_{13}^b = 0.07, m_{21}^b = 0.24, m_{22}^b = 0.27, m_{23}^b = 0.1, m_{11}^v = 1.67, m_{12}^v = 0.45, m_{13}^v = 0.34, m_{21}^v = 0.67, m_{22}^v = 0.26, m_{23}^v = 0.34$. The conditions $(C1)$–$(C7)$ of Theorem 1 hold for the network (8) with $K_{ij} = 1$, for all $i = 1,2$, $j = 1,2,3$, $L = 0.5$, $\lambda_{11} = 3\pi, \lambda_{12} = 2\pi, \lambda_{13} = 4\pi, \lambda_{21} = 5\pi, \lambda_{22} = 3\pi, \lambda_{23} = 2\pi$. As is the case for Theorem 1, Equation (8) admits a unique asymptotically Poisson stable solution $z(t) = (z_{ij}(t)), i = 1,2, j = 1,2,3$. In Figure 1, the solution $x(t) = (x_{ij}(t)), i = 1,2$, $j = 1,2,3$, of SICNNs (8) is shown, which asymptotically converges to $z(t)$.

Figure 2 depicts the coordinates $x_{11} - x_{12} - x_{13}$ of the solution of (8).

To emphasize the role of the variable passive rates for the behavior of the outputs, in the next simulations, we consider the constant and Poisson stable components of the passive rates. In Figure 3, the outputs of the neural network (8) with $a_{11}(t) + b_{11}(t) = 3$, $a_{12}(t) + b_{12}(t) = 2$, $a_{13}(t) + b_{13}(t) = 4$, $a_{21}(t) + b_{21}(t) = 5$, $a_{22}(t) + b_{22}(t) = 3$, $a_{23}(t) + b_{23}(t) = 6$ are demonstrated. One can observe that the constancy is combined with the irregular contribution of the inputs.

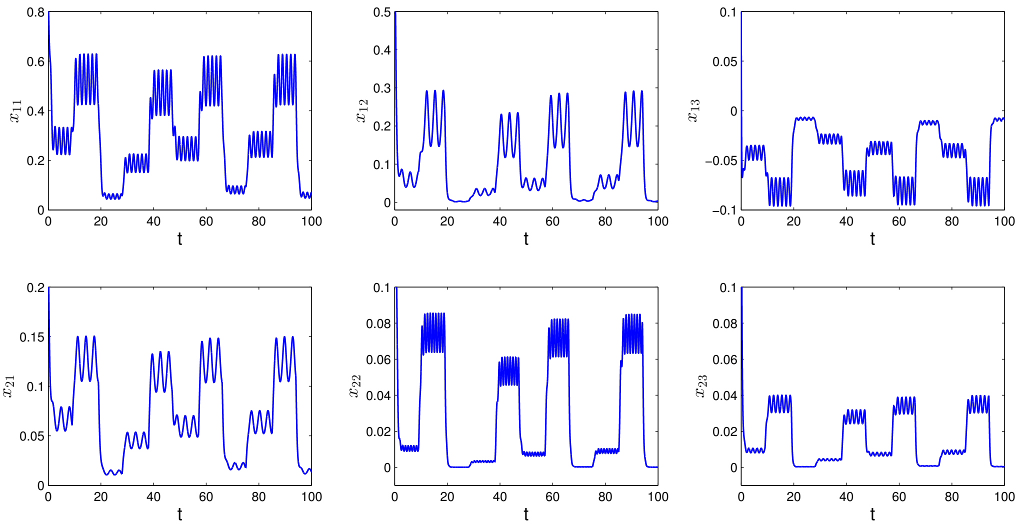

Figure 1. The solution $x(t) = (x_{ij}(t))$, $i = 1, 2$, $j = 1, 2, 3$, of the neural network (8) with the degree of periodicity $\kappa = 1/3$ and the initial values $x_{11}(0) = 0.8$, $x_{12}(0) = 0.5$, $x_{13}(0) = 0.1$, $x_{21}(0) = 0.2$, $x_{22}(0) = 0.1$, $x_{23}(0) = 0.1$.

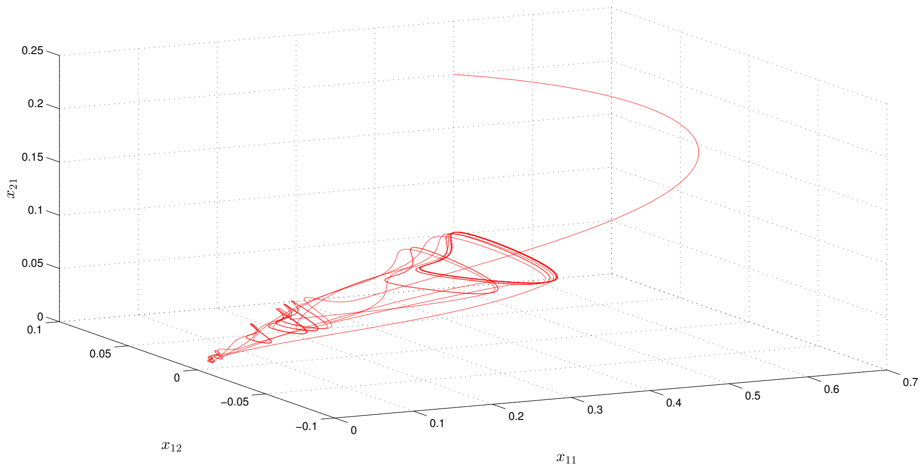

Figure 2. The coordinates $x_{11} - x_{12} - x_{13}$ of the solution $x(t) = (x_{ij}(t))$, $i = 1, 2$, $j = 1, 2, 3$, of the neural network (8) with the degree of periodicity $\kappa = 1/3$ and the initial values $x_{11}(0) = 0.8$, $x_{12}(0) = 0.5$, $x_{13}(0) = 0.1$, $x_{21}(0) = 0.2$, $x_{22}(0) = 0.1$, $x_{23}(0) = 0.1$.

Example 2. *Now, we consider SICNNs (8) where $i = 1, 2$, $j = 1, 2, 3$, activation function $f(s) = 0.5arctan(s)$, the coupling strength $C_{ij}^{11} = 0.04$, $C_{ij}^{12} = 0.03$, $C_{ij}^{13} = 0.05$, $C_{ij}^{21} = 0.01$, $C_{ij}^{22} = 0.06$, $C_{ij}^{23} = 0.02$. For each fixed $k = 1, 2$, and $l = 1, 2, 3$, the coefficients C_{ij}^{kl} are the same for all i, j, such that the cell C_{kl} belongs to $N_1(i, j)$. Functions $a_{ij}(t)$ are π-periodic such that $a_{11}(t) = 3 + \cos(4t)$, $a_{12}(t) = 2 + \sin(2t)$, $a_{13}(t) = 4 + \sin(4t)$, $a_{21}(t) = 5 + \cos(2t)$, $a_{22}(t) = 3 + \sin(6t)$, $a_{23}(t) = 6 + \sin(4t)$. The functions $b_{ij}(t)$ and $v_{ij}(t)$ are Poisson stable such that $b_{11}(t) = 0.5\Theta(t)$, $b_{12}(t) = 0.3\Theta(t)$, $b_{13}(t) = 0.2\Theta(t)$, $b_{21}(t) = 0.7\Theta(t)$, $b_{22}(t) = 0.8\Theta(t)$, $b_{23}(t) = 0.3\Theta(t)$, $v_{11}(t) = \sin(0.2t) + 0.5\Theta(t)$, $v_{12}(t) = \sin(0.4t) + 0.4\Theta^2(t)$, $v_{13}(t) = \cos(0.1t) - 0.1\Theta(t)$, $v_{21}(t) = \sin(0.2t) + 0.2\Theta(t)$, $v_{22}(t) = \cos(0.2t) + 0.7\Theta^3(t)$, $v_{23}(t) = \cos(0.1t) + 0.2\Theta^2(t)$, where $\Theta(t)$ is the solution of Equation (7) with the step of length $h = \pi/10$. The common period of the functions $a_{ij}(t)$ and $v_{ij}(t)$ equals to 20π, and the degree of periodicity is equal to $\kappa = 200$. Figure 4 depicts simulation results of SICNNs (8) with initial values $x_{11}(0) = 0.8$, $x_{12}(0) = 0.5$, $x_{13}(0) = 0.1$, $x_{21}(0) = 0.2$, $x_{22}(0) = 0.1$, $x_{23}(0) = 0.1$. The coordinates $x_{11} - x_{12} - x_{13}$ of the trajectory with the same initial data are shown in Figure 5.*

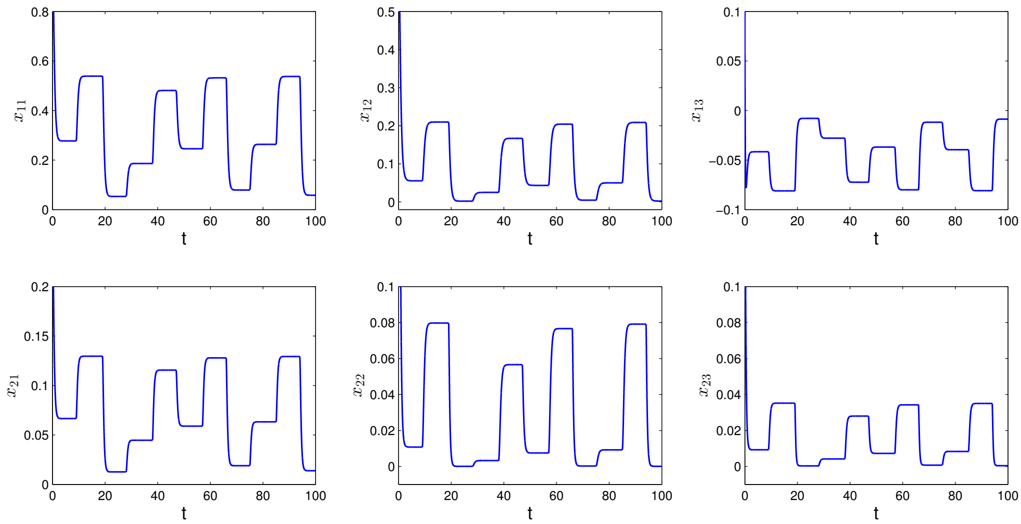

Figure 3. The solution $x(t) = (x_{ij}(t))$, $i = 1,2$, $j = 1,2,3$, of the neural network (8) with constant passive decay rates and initial values $x_{11}(0) = 0.8$, $x_{12}(0) = 0.5$, $x_{13}(0) = 0.1$, $x_{21}(0) = 0.2$, $x_{22}(0) = 0.1$, $x_{23}(0) = 0.1$. The degree of periodicity $\kappa = 1/3$.

Comparing Figures 1 and 4, one can understand the importance of the periodicity degree for the models. That is, the periodicity characteristic is seen to be better if the degree is larger than one, and the Poisson stability is better visualized for κ smaller than one. This is why $\kappa = 1$ is the center of antisymmetry for degree of periodicity.

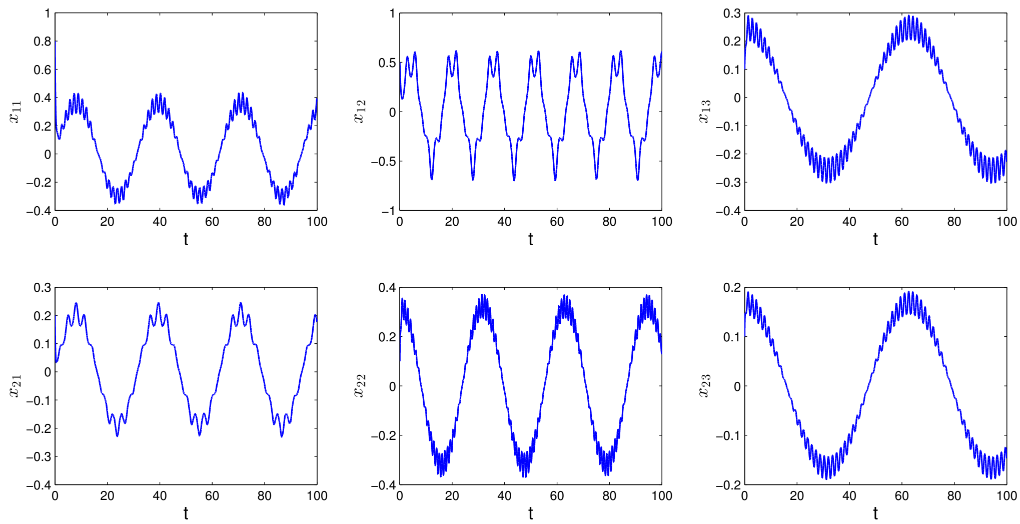

Figure 4. The solution $x(t) = (x_{ij}(t))$, $i = 1,2$, $j = 1,2,3$, of the neural network (8) with the degree of periodicity $\kappa = 200$ and the initial values $x_{11}(0) = 0.8$, $x_{12}(0) = 0.5$, $x_{13}(0) = 0.1$, $x_{21}(0) = 0.2$, $x_{22}(0) = 0.1$, $x_{23}(0) = 0.1$.

Example 3. *Let us consider the following neural network*

$$\frac{dy_{ij}}{dt} = -(a_{ij}(t) + b_{ij}(t))y_{ij} - \sum_{C_{kl} \in N_1(i,j)} C_{ij}^{kl} f(y_{kl}) y_{ij} + v_{ij}(t), \tag{9}$$

where $i = 1,2$, $j = 1,2,3$, *activation function* $f(s) = 0.25 tanh(s)$, *the coupling strength* $C_{ij}^{11} = 0.003$, $C_{ij}^{12} = 0.002$, $C_{ij}^{13} = 0$, $C_{ij}^{21} = 0.005$, $C_{ij}^{22} = 0.004$, $C_{ij}^{23} = 0.001$. *For each fixed* $k = 1,2$ *and* $l = 1,2,3$, *the coefficients* C_{ij}^{kl} *are the same for all* i,j *such that the cell* C_{kl} *belongs to* $N_1(i,j)$. *The functions* $a_{ij}(t)$ *are* 2*-periodic such that* $a_{11}(t) = 4 + \cos(2\pi t)$,

$a_{12}(t) = 4 + \sin(5\pi t)$, $a_{13}(t) = 3 + \sin(4\pi t)$, $a_{21}(t) = 5 + \cos(4\pi t)$, $a_{22}(t) = 5 + \sin(2\pi t)$, $a_{23}(t) = 3 + \sin(\pi t)$. *Functions* $b_{ij}(t)$ *and* $v_{ij}(t)$ *are Poisson stable,* $b_{11}(t) = 0.1x_{11}(t)$, $b_{12}(t) = 0.4x_{21}(t)$, $b_{13}(t) = 0.3x_{13}(t)$, $b_{21}(t) = 0.6x_{22}(t)$, $b_{22}(t) = 0.4x_{12}(t)$, $b_{23}(t) = 0.5x_{23}(t)$, $v_{11}(t) = 0.2x_{12}(t)$, $v_{12}(t) = 0.4x_{22}(t)$, $v_{13}(t) = 0.6x_{21}(t)$, $v_{21}(t) = 0.2x_{13}(t)$, $v_{22}(t) = 0.5x_{11}(t)$, $v_{23}(t) = 0.3x_{22}(t)$. *The function* $x(t) = (x_{ij}(t))$, $i = 1,2$, $j = 1,2,3$ *is the solution of SICNNs (8) obtained for* $\Theta(t)$ *with* $h = 2$. *In Figure 6, the solution* $y(t) = (y_{ij}(t))$, $i = 1,2$, $j = 1,2,3$, *of (9) with* $y_{11}(0) = 0.05$, $y_{12}(0) = 0.01$, $y_{13}(0) = 0.04$, $y_{21}(0) = 0$, $y_{22}(0) = 0.07$, $y_{23}(0) = 0.03$, *is depicted. In the model, the periodicity degree is equal to* 1 *and the periodicity is clearly not observable.*

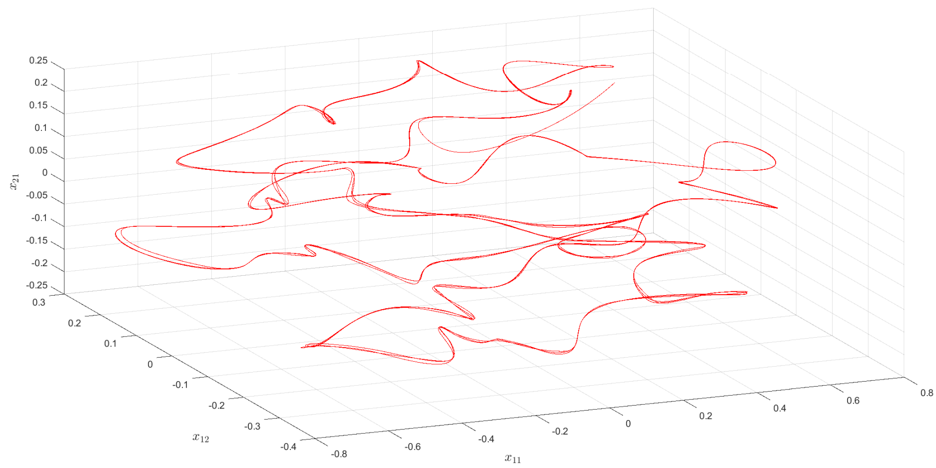

Figure 5. The coordinates $x_{11} - x_{12} - x_{13}$ of the trajectory $x(t) = (x_{ij}(t))$, $i = 1,2$, $j = 1,2,3$, of the neural network (8). The degree of periodicity is equal to 200.

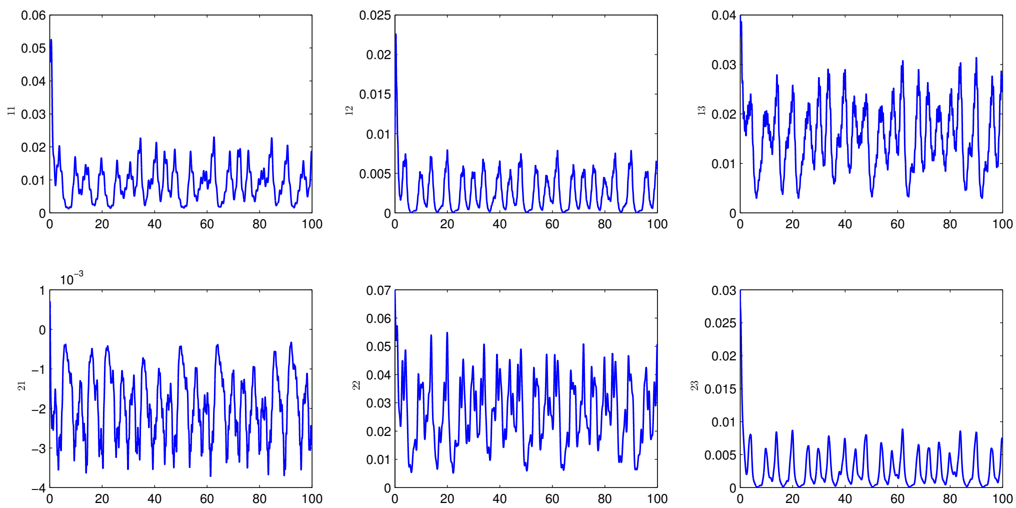

Figure 6. The solution $y(t) = (y_{ij}(t))$, $i = 1,2$, $j = 1,2,3$, of the SICNNs (9), with a degree of periodicity $\kappa = 1$ and initial data $y_{11}(0) = 0.05$, $y_{12}(0) = 0.01$, $y_{13}(0) = 0.04$, $y_{21}(0) = 0$, $y_{22}(0) = 0.07$, $y_{23}(0) = 0.03$.

4. Discussion

In this part of the paper, we provide the ideas behind the theoretical research of the dynamics of neural networks which are useful for applications in engineering. We found that the simulations of our study are similar to those modeled by neural networks in industrial problems. For example, consider tracking of periodical or square waves dynamics. We are confident that one should better learn what can happen in the dynamics of neural networks with a sophisticated environment and structure. Furthermore, the information of the paper is useful in that sense. One can assume that in addition to the tracking periods, amplitudes of the periodical and square wave dynamics, the neural networks' motions can also be considered for the Poisson sequences. Thus, the instruments for synchronization and control can be significantly improved, if one consider our proposals.

To shed more light for the suggestions and provide several issues for the next observations, let us look not only at the simulations results for the networks in the examples above but simulations for Poisson stable functions, especially driven to compare with the industrial simulations in papers [50–54]. For this reason, let us consider the two-component function $F(t,\kappa) = a\cos(\frac{2\pi t}{\omega}) + b\Theta(t)$, where a and b are real coefficients, $\Theta(t)$ is the Poisson stable function with step h described in the last section, and the first component is an ω-periodic function. The parameter κ is the periodicity degree, which was introduced above in Example 1. It can be very useful for the analysis of time series obtained in different areas—both theoretical and engineering. In Figures 7–9, we have the graphs of functions $F(t,80), F(t,1/5)$ and $F(t,1)$, respectively. The graph of function $F(t,80)$ with the periodicity degree $\kappa > 1$ is shown in Figure 7. We obtain the function that admits a clear periodic shape which is enveloped by irregular Poisson stability—which can be said about the dominance of periodicity in this case.

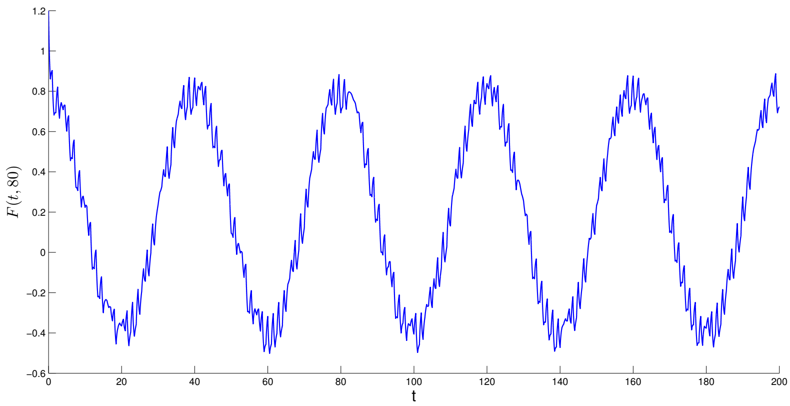

Figure 7. The graph of function $F(t,80)$ with $a = 0.6$, $b = 1$, $\omega = 40$, $\kappa = 80$.

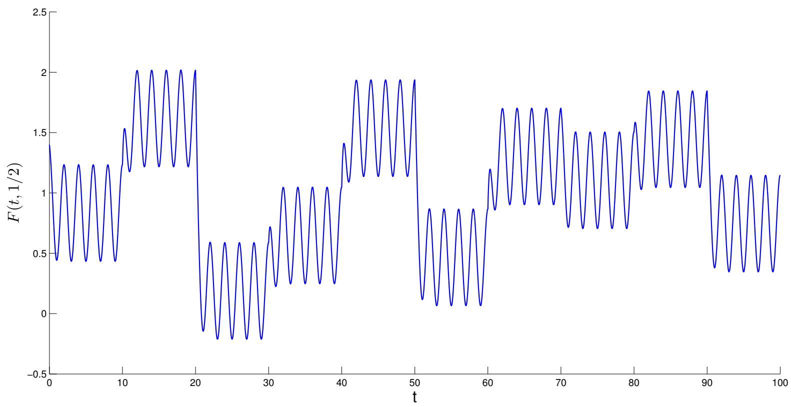

Figure 8. The graph of function $F(t,1/5)$ with $a = 0.4$, $b = 5$, $\omega = 2$, $\kappa = 1/5$.

For the function $F(t,1/5)$, where $\kappa < 1$, and observing its graph in Figure 8, we have the opposite effect, when the irregular stability dominates and the periodicity, which appears locally on separated intervals, envelopes the Poisson stability.

If $\kappa = 1$, then the graph of function $F(t,1)$ in Figure 9 demonstrates that both phenomena—periodicity and Poisson stability—are equally present in the dynamics.

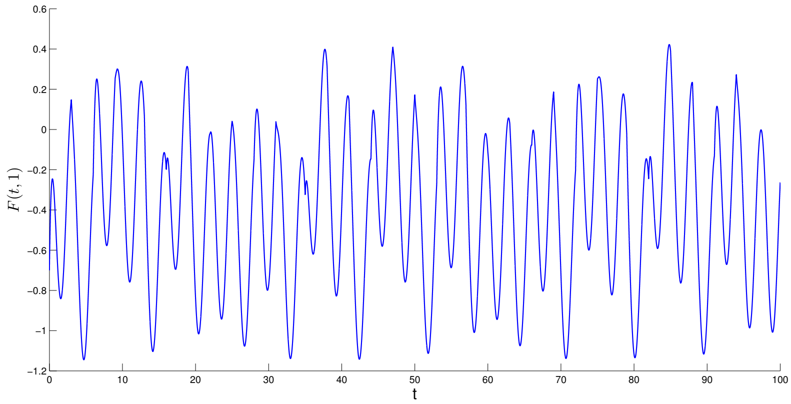

Figure 9. The graph of function $F(t, 1)$ with $a = 0.5$, $b = -2$, $\omega = \pi$, $\kappa = 1$.

To estimate the future prospects of our suggestions, the simulations of the paper were compared with some industrial applications of neural networks. First of all, it was found that examples from an historical hourly weather dataset, Figure 9 in [50], had the same shape as the solution $x(t) = (x_{ij}(t))$, $i = 1, 2$, $j = 1, 2, 3$, of neural network (8) with the periodicity degree $\kappa = 200$ and the initial values $x_{11}(0) = 0.8$, $x_{12}(0) = 0.5$, $x_{13}(0) = 0.1$, $x_{21}(0) = 0.2$, $x_{22}(0) = 0.1$, $x_{23}(0) = 0.1$ in Figure 4. Moreover, it is very similar to the graph of function $F(t, 80)$ in Figure 7. It is remarkable that both mathematical objects are with $\kappa > 1$. It is important that the dominance is numerically indicated for the value of the periodicity degree larger than one.

Our observations then relate to the values of the degree less than one. In Figure 8 of the paper [51] (track control of 1 Hz square wave (no load)), one can see oscillations similar to Poisson stable motions with $\kappa < 1$ in Figures 1 and 8, which are obtained on the basis of our theoretical issues. Analyzing simulations with a periodicity degree smaller than one, one can say that there is a loss of periodicity and dominance of irregularity, which is specified as Poisson stability, while the result in [51] might be accepted as coexistence of the square wave periodicity and the Poisson stability in our comprehension. Nevertheless, we believe that one can use the present theoretical results for qualitative characteristics of the square wave tracking with SICNNs [52,53].

Figure 36(a) in [54] is very similar to our simulations in Figures 6 and 9 with the unit degree of periodicity. This confirms that specific Poisson stable motions can be useful to represent the dynamics of linear and nonlinear single-degree-of-freedom systems, as well as full-scale three-story multi-degree of freedom steel frame [54].

5. Conclusions

In this paper, we considered SICNNs with variable two-component rates and Poisson stable inputs. Sufficient conditions were established to provide the existence of Poisson stable solutions for the SICNNs. The line of periodic, almost periodic and recurrent oscillations in neural networks is continued. Introducing the concept of the degree of periodicity, we showed by examples how it affects the dynamics of neural networks. The suggestions are constructive and suitable for simulations.

Author Contributions: M.A.: conceptualization; methodology; investigation. M.T.: investigation; supervision; writing—review and editing. A.Z.: software; investigation; writing—original draft. All authors have read and agreed to the published version of the manuscript.

Funding: M. Tleubergenova and A. Zhamanshin have been supported by the Science Committee of the Ministry of Education and Science of the Republic of Kazakhstan (grant No. AP08856170 and No. AP09258737). M. Akhmet and A. Zhamanshin have been supported by 2247-A National Leading Researchers Program of TUBITAK, Turkey, N 120C138.

Institutional Review Board Statement: Not applicable.

Informed Consent Statement: Not applicable.

Data Availability Statement: Not applicable.

Acknowledgments: The authors are very thankful to the editor and referees for their valuable comments and suggestions.

Conflicts of Interest: The authors declare no conflict of interest.

Appendix A

In what follows, the basic constructive properties of the operator Π are provided, which are needed to prove Theorem 1.

Lemma A1. *Suppose that assumptions (C1)–(C7) are true. Then, operator* Π *is invariant in the set* $\mathcal{B}$.

Proof. Let a function $\phi(t)$ belong to $\mathcal{B}$, then we obtain

$$
\begin{aligned}
&|\Pi_{ij}\phi(t)| \leq |\int_{-\infty}^{t} e^{-\int_s^t \alpha_{ij}(u)du}\Big(b_{ij}(s)\phi_{ij}(s) + \sum_{C_{kl}\in N_r(i,j)} C_{ij}^{kl} f(\phi_{kl})(s)\phi_{ij}(s) - v_{ij}(s)\Big)ds| \leq \\
&\int_{-\infty}^{t} K_{ij}e^{-\lambda_{ij}(t-s)}\Big(|b_{ij}(s)||\phi_{ij}(s)| + \sum_{C_{kl}\in N_r(i,j)} C_{ij}^{kl}|f(\phi_{kl})(s)||\phi_{ij}(s)| + |v_{ij}(s)|\Big)ds \leq \qquad \text{(A1)}\\
&\frac{K_{ij}}{\lambda_{ij}}(m_{ij}^{b}H + m_f H \sum_{C_{kl}\in N_r(i,j)} C_{ij}^{kl} + m_{ij}^{v}),
\end{aligned}
$$

for all $i = 1,2,\ldots,m, j = 1,2,\ldots,n$. By conditions (C6) and (C7), we obtain that $|\Pi_{ij}\phi(t)| < H, i = 1,2,\ldots,m, j = 1,2,\ldots,n$.

We then show that $\Pi_{ij}\phi(t)$, $i = 1,2,\ldots,m$, $j = 1,2,\ldots,n$, are Poisson stable functions. Consider a fixed number $\epsilon > 0$ and bounded interval $[\alpha,\beta] \subset \mathbb{R}$. One can choose numbers γ, ξ such that $\alpha > \gamma$ and $\xi > 0$ which obey the following relations,

$$
\frac{2K_{ij}}{\lambda_{ij}}e^{-\lambda_{ij}(\alpha-\gamma)}(m_f H \sum_{C_{kl}\in N_r(i,j)} C_{ij}^{kl} + m_{ij}^{b}H + m_{ij}^{v}) < \frac{\epsilon}{4}, \tag{A2}
$$

$$
\frac{K_{ij}}{\lambda_{ij}}((2LH^2 + 2Hm_f)\sum_{C_{kl}\in N_r(i,j)} C_{ij}^{kl} + 2m_{ij}^{b}H + 2m_{ij}^{v})e^{-\lambda_{ij}(\alpha-\gamma)} < \frac{\epsilon}{4}, \tag{A3}
$$

$$
\frac{K_{ij}}{\lambda_{ij}}(e^{\xi(\beta-\gamma)} - 1)(m_f H \sum_{C_{kl}\in N_r(i,j)} C_{ij}^{kl} + m_{ij}^{b}H + m_{ij}^{v}) < \frac{\epsilon}{4}, \tag{A4}
$$

$$
\frac{K_{ij}\xi}{\lambda_{ij}}((LH + m_f)\sum_{C_{kl}\in N_r(i,j)} C_{ij}^{kl} + H + m_{ij}^{b} + 1) < \frac{\epsilon}{4}, \tag{A5}
$$

for all $i = 1,2,\ldots,m$, $j = 1,2,\ldots,n$. Since the interval $[\alpha,\beta] \subset [\gamma,\beta]$, the present technique of discussion is called the method of included intervals.

Because the functions $b_{ij}(t)$ and $v_{ij}(t)$, $i = 1,2,\ldots,m$, $j = 1,2,\ldots,n$, are Poisson stable, the function $\phi(t) = (\phi_{ij}(t))$, $i = 1,2,\ldots,m$, $j = 1,2,\ldots,n$, belongs to $\mathcal{B}$, whilst the convergence sequence, t_p, is common for all of them, and the Poisson number κ_ω is equal to zero, by Lemma A2 in [32], it is true that $|b_{ij}(t+t_p) - b_{ij}(t)| < \xi$, $|v_{ij}(t+t_p) - v_{ij}(t)| < \xi$, $|\phi_{ij}(t+t_p) - \phi_{ij}(t)| < \xi$ for $t \in [\gamma,\beta]$, and $|a_{ij}(t+t_p) - a_{ij}(t)| < \xi$ for $t \in \mathbb{R}$, sufficiently large p and $i = 1,2,\ldots,m$, $j = 1,2,\ldots,n$. We have that

$$|\Pi_{ij}\phi(t+t_p) - \Pi_{ij}\phi(t)| \le | \int_{-\infty}^{t} e^{-\int_s^t a_{ij}(u+t_p)du}\Big(b_{ij}(s+t_p)\phi_{ij}(s+t_p) +$$
$$\sum_{C_{kl}\in N_r(i,j)} C_{ij}^{kl} f(\phi_{kl}(s+t_p))\phi_{ij}(s+t_p) - v_{ij}(s+t_p)\Big)ds +$$
$$\int_{-\infty}^{t} e^{-\int_s^t a_{ij}(u)du}\Big(b_{ij}(s)\phi_{ij}(s) + \sum_{C_{kl}\in N_r(i,j)} C_{ij}^{kl} f(\phi_{kl}(s))\phi_{ij}(s) - v_{ij}(s)\Big)ds| \le$$
$$\int_{-\infty}^{t} |e^{-\int_s^t a_{ij}(u+t_p)du} - e^{-\int_s^t a_{ij}(u)du}|\Big(|b_{ij}(s+t_p)\phi_{ij}(s+t_p) +$$
$$\sum_{C_{kl}\in N_r(i,j)} C_{ij}^{kl} f(\phi_{kl}(s+t_p))\phi_{ij}(s+t_p) - v_{ij}(s+t_p)|\Big)ds +$$
$$\int_{-\infty}^{t} e^{-\int_s^t a_{ij}(u)du}\Big(|b_{ij}(s+t_p)\phi_{ij}(s+t_p) - b_{ij}(s)\phi_{ij}(s) +$$
$$\sum_{C_{kl}\in N_r(i,j)} C_{ij}^{kl}(f(\phi_{kl}(s+t_p))\phi_{ij}(s+t_p) - f(\phi_{kl}(s))\phi_{ij}(s)) - v_{ij}(s+t_p) + v_{ij}(s)|\Big)ds.$$

Let us present the sum of integrals in the last inequality as $I_1 + I_2$, such that

$$I_1 = \int_{-\infty}^{\gamma} |e^{-\int_s^t a_{ij}(u+t_p)du} - e^{-\int_s^t a_{ij}(u)du}|\Big(|b_{ij}(s+t_p)\phi_{ij}(s+t_p) +$$
$$\sum_{C_{kl}\in N_r(i,j)} C_{ij}^{kl} f(\phi_{kl}(s+t_p))\phi_{ij}(s+t_p) - v_{ij}(s+t_p)|\Big)ds +$$
$$\int_{-\infty}^{\gamma} e^{-\int_s^t a_{ij}(u)du}\Big(|b_{ij}(s+t_p)\phi_{ij}(s+t_p) - b_{ij}(s)\phi_{ij}(s) +$$
$$\sum_{C_{kl}\in N_r(i,j)} C_{ij}^{kl}(f(\phi_{kl}(s+t_p))\phi_{ij}(s+t_p) - f(\phi_{kl}(s))\phi_{ij}(s)) - v_{ij}(s+t_p) + v_{ij}(s)|\Big)ds,$$

and

$$I_2 = \int_{\gamma}^{t} |e^{-\int_s^t a_{ij}(u+t_p)du} - e^{-\int_s^t a_{ij}(u)du}|\Big(|b_{ij}(s+t_p)\phi_{ij}(s+t_p) +$$
$$\sum_{C_{kl}\in N_r(i,j)} C_{ij}^{kl} f(\phi_{kl}(s+t_p))\phi_{ij}(s+t_p) - v_{ij}(s+t_p)|\Big)ds +$$
$$\int_{\gamma}^{t} e^{-\int_s^t a_{ij}(u)du}\Big(|b_{ij}(s+t_p)\phi_{ij}(s+t_p) - b_{ij}(s)\phi_{ij}(s) +$$
$$\sum_{C_{kl}\in N_r(i,j)} C_{ij}^{kl}(f(\phi_{kl}(s+t_p))\phi_{ij}(s+t_p) - f(\phi_{kl}(s))\phi_{ij}(s)) - v_{ij}(s+t_p) + v_{ij}(s)|\Big)ds.$$

One can find that

$$I_1 \le \int_{-\infty}^{\gamma} 2K_{ij}e^{-\lambda_{ij}(t-s)}\Big(m_{ij}^b H + \sum_{C_{kl}\in N_r(i,j)} C_{ij}^{kl} m_f H + m_{ij}^v\Big)ds +$$
$$\int_{-\infty}^{\gamma} K_{ij}e^{-\lambda_{ij}(t-s)}\Big(2m_{ij}^b H + \sum_{C_{kl}\in N_r(i,j)} C_{ij}^{kl}(2LH^2 + 2Hm_f) + 2m_{ij}^v\Big)ds,$$

and

$$I_2 \le \int_{\gamma}^{t} K_{ij}e^{-\lambda_{ij}(t-s)}(e^{\xi(\beta-\gamma)} - 1)\Big(m_{ij}^b H + \sum_{C_{kl}\in N_r(i,j)} C_{ij}^{kl} m_f H + m_{ij}^v\Big)ds +$$
$$\int_{\gamma}^{t} K_{ij}e^{-\lambda(t-s)}\Big(m_{ij}^b\xi + H\xi + \sum_{C_{kl}\in N_r(i,j)} C_{ij}^{kl}(LH\xi + m_f\xi) + \xi\Big)ds.$$

Now, applying inequalities (A2)–(A5), we obtain that the following estimates are correct for each $i = 1, 2, \dots, m, j = 1, 2, \dots, n$:

$$I_1 \leq \frac{2K_{ij}}{\lambda_{ij}} e^{-\lambda_{ij}(\alpha-\gamma)}(m_{ij}^b H + m_f H \sum_{C_{kl}\in N_r(i,j)} C_{ij}^{kl} + m_{ij}^v) +$$
$$\frac{K_{ij}}{\lambda_{ij}}((2LH^2 + 2Hm_f) \sum_{C_{kl}\in N_r(i,j)} C_{ij}^{kl} + 2m_{ij}^b H + 2m_{ij}^v) e^{-\lambda_{ij}(\alpha-\gamma)} < \frac{\epsilon}{4} + \frac{\epsilon}{4} = \frac{\epsilon}{2}, \quad \text{(A6)}$$

and

$$I_2 \leq \frac{K_{ij}}{\lambda_{ij}}(e^{\xi(\beta-\gamma)} - 1)(m_{ij}^b H + m_f H \sum_{C_{kl}\in N_r(i,j)} C_{ij}^{kl} + m_{ij}^v) +$$
$$\frac{K_{ij}}{\lambda_{ij}}((LH\xi + m_f\xi) \sum_{C_{kl}\in N_r(i,j)} C_{ij}^{kl} + m_{ij}^b\xi + H\xi + \xi) < \frac{\epsilon}{4} + \frac{\epsilon}{4} = \frac{\epsilon}{2}. \quad \text{(A7)}$$

From inequalities (A6) and (A7) it follows that $|\Pi_{ij}\phi(t + t_p) - \Pi_{ij}\phi(t)| \leq I_1 + I_2 < \epsilon$ for $t \in [\alpha, \beta]$, and all $i = 1, 2, \dots, m, j = 1, 2, \dots, n$. Therefore, $\Pi\mathcal{B} \subseteq \mathcal{B}$. □

Lemma A2. *Assumptions (C1) and (C4)–(C6) imply that* Π *is a contraction operator in* $\mathcal{B}$.

Proof. Let us take two functions φ and ψ that belong to $\mathcal{B}$. It is true that for fixed i and j that the inequality

$$|\Pi_{ij}\varphi(t) - \Pi_{ij}\psi(t)| \leq \int_{-\infty}^{t} e^{-\int_s^t a_{ij}(u)du}\Big(|b_{ij}(s)||\varphi_{ij}(s) - \psi_{ij}(s)| +$$
$$\sum_{C_{kl}\in N_r(i,j)} C_{ij}^{kl}(|f(\varphi_{kl}(s))\varphi_{ij}(s) - f(\varphi_{kl}(s))\psi_{ij}(s)| + |f(\varphi_{kl}(s))\psi_{ij}(s) - f(\psi_{kl}(s))\psi_{ij}(s))|\Big)ds \leq$$
$$\frac{K_{ij}}{\lambda_{ij}}\Big(m_{ij}^b + (m_f + LH)\sum_{C_{kl}\in N_r(i,j)} C_{ij}^{kl}\Big)\|\varphi - \psi\|_0$$

is valid. This is why $\|\Pi\varphi - \Pi\psi\|_0 \leq \dfrac{K_{ij}(m_{ij}^b + (m_f + LH)\sum_{C_{kl}\in N_r(i,j)} C_{ij}^{kl})}{\lambda_{ij}}\|\varphi - \psi\|_0$. By condition $(C6)$, the operator Π is a contraction in $\mathcal{B}$. □

References

1. Chua, L.; Yang, L. Cellular neural networks: Applications. *IEEE Trans. Circuits Syst.* **1988**, *35*, 1273–1290. [CrossRef]
2. Bouzerdoum, A.; Pinter, R. Shunting inhibitory cellular neural networks: Derivation and stability analysis. *IEEE Trans. Circuits Syst. I Fundam. Theory Appl.* **1993**, *40*, 215–221. [CrossRef]
3. Li, Y.; Wang, L.; Fei, Y. Periodic Solutions for Shunting Inhibitory Cellular Neural Networks of Neutral Type with Time-Varying Delays in the Leakage Term on Time Scales. *J. Appl. Math.* **2014**, *2014*, 496396. [CrossRef]
4. Huang, C.; Wen, S.; Huang, L. Dynamics of anti–periodic solutions on shunting inhibitory cellular neural networks with multi-proportional delays. *Neurocomputing* **2019**, *357*, 47–52. [CrossRef]
5. Peng, G.; Li, L. Anti–periodic solutions for shunting inhibitory cellular neural networks with continuously distributed delays. *Nonlinear Anal. Real World Appl.* **2009**, *10*, 2434–2440. [CrossRef]
6. Ou, C. Almost periodic solutions for shunting inhibitory cellular neural networks. *Nonlinear Anal. Real World Appl.* **2019**, *10*, 2652–2658. [CrossRef]
7. Li, Y.; Meng, X. Almost periodic solutions for quaternion-valued shunting inhibitory cellular neural networks of neutral type with time delays in the leakage term. *Int. J. Syst. Sci.* **2018**, *49*, 2490–2505. [CrossRef]
8. Li, Y.; Wang, C. Almost periodic solutions of shunting inhibitory cellular neural networks on time scales. *Commun. Nonlinear Sci. Numer. Simul.* **2018**, *17*, 3258–3266. [CrossRef]
9. Lu, Y.; Ji, D. Pseudo almost periodic solutions for shunting inhibitory cellular neural networks with continuously distributed delays. *J. Inequalities Appl.* **2017**, *2017*, 242. [CrossRef]
10. Zhang, A. Pseudo Almost Periodic Solutions for SICNNs with Oscillating Leakage Coefficients and Complex Deviating Arguments. *Neural Process. Lett.* **2017**, *45*, 183–196. [CrossRef]

11. Sell, G. *Topological Dynamics and Ordinary Differential Equations*; Van Nostrand Reinhold Company: London, UK, 1971.
12. Poincare, H. *New Methods of Celestial Mechanics*; Dover Publications: New York, NY, USA, 1957.
13. Birkhoff, G. *Dynamical Systems*; American Mathematical Society: Providence, RI, USA, 1927.
14. Nayfeh, A.; Mook, D. *Nonlinear Oscillations*; Wiley: New York, NY, USA, 1979.
15. Hoppensteadt, F.; Izhikevich, E. *Weakly Connected Neural Networks*; Springer: New York, NY, USA, 1997.
16. Fink, A. *Almost Periodic Differential Equations*; Springer: New York, NY, USA, 1974.
17. Levitan, B.; Zhikov, V. *Almost Periodic Functions and Differential Equations*; Cambridge University Press: Cambridge, UK, 1983.
18. Corduneanu, C. *Almost Periodic Oscillations and Waves*; Springer: New York, NY, USA, 2009.
19. Besicovitch, A. *Almost Periodic Functions*; Dover: Cambridge, UK, 1954.
20. Liu, B. Almost periodic solutions for Hopfield neural networks with continuously distributed delays. *Math. Comput. Simul.* **2007**, *73*, 327–335. [CrossRef]
21. Cao, J. New results concerning exponential stability and periodic solutions of delayed cellular neural networks. *Phys. Lett. A* **2003**, *307*, 136–147. [CrossRef]
22. Zhang, L.; Du, B. Periodic solution for inertial neural networks with variable parameters. *AIMS Math.* **2021**, *6*, 13580–13591. [CrossRef]
23. Xu, C.; Pang, Y.; Li, P. Anti–periodic solutions of Cohen-Grossberg shunting inhibitory cellular neural networks on time scales. *J. Nonlinear Sci. Appl.* **2016**, *9*, 2376–2388. [CrossRef]
24. Huang, Z. Almost periodic solutions for fuzzy cellular neural networks with multi-proportional delays. *Int. J. Mach. Learn. Cybern.* **2017**, *8*, 1323–1331. [CrossRef]
25. Bender, P. Recurrent solutions to systems of ordinary differential equations. *J. Differ. Equ.* **1969**, *5*, 271–282. [CrossRef]
26. Kumar, A.; Bhagat, R. Poisson stability in product of dynamical systems. *Int. J. Math. Math. Sci.* **1987**, *10*, 613–614. [CrossRef]
27. Hino, Y. Recurrent solutions for linear almost periodic systems. *Funkc. Ekvacioj* **1985**, *28*, 117–119.
28. Knight, R. Recurrent and Poisson stable flows. *Proc. Am. Math. Soc.* **1981**, *83*, 49–53. [CrossRef]
29. Holmes, P. Poincare, celestial mechanics, dynamical-systems theory and chaos. *Phys. Rep.* **1990**, *193*, 137–163. [CrossRef]
30. Akhmet, M.; Tleubergenova, M.; Zhamanshin, A. Poincare chaos for a hyperbolic quasilinear system. *Miskolc Math. Notes* **2019**, *20*, 33–44. [CrossRef]
31. Akhmet, M.; Tleubergenova, M.; Zhamanshin, A. Quasilinear differential equations with strongly unpredictable solutions. *Carpathian J. Math.* **2020**, *36*, 341–349. [CrossRef]
32. Akhmet, M.; Tleubergenova, M.; Zhamanshin, A. Modulo periodic Poisson stable solutions of quasilinear differential equations. *Entropy* **2021**, *23*, 1535. [CrossRef] [PubMed]
33. Akhmet, M.; Seilova, R.; Tleubergenova, M.; Zhamanshin, A. Shunting inhibitory cellular neural networks with strongly unpredictable oscillations. *Commun. Nonlinear Sci. Numer. Simul.* **2020**, *89*, 105287. [CrossRef]
34. Akhmet, M.; Tleubergenova, M.; Zhamanshin, A. Inertial neural networks with unpredictable oscillations. *Mathematics* **2020**, *8*, 1797. [CrossRef]
35. Akhmet, M.; ÇinÇin, D.A.; Tleubergenova, M.; Nugayeva, Z. Unpredictable oscillations for Hopfield–type neural networks with delayed and advanced arguments. *Mathematics* **2020**, *9*, 571. [CrossRef]
36. Akhmet, M. *Domain Structured Dynamics: Unpredictability, Chaos, Randomness, Fractals, Differential Equations and Neural Networks*; IOP Publishing: Bristol, UK, 2021.
37. Shcherbakov, B.A. Classification of Poisson—stable motions. Pseudo—recurrent motions. *Dokl Akad Nauk. SSSR* **1962**, *146*, 322–324.
38. Shcherbakov, B.A. Poisson stable solutions of differential equations, and topological dynamics. *Differ. Uravn* **1969**, *5*, 2144–2155.
39. Cheban, D.; Liu, Z. Poisson stable motions of monotone nonautonomous dynamical systems. *Sci. China Math.* **2019**, *62*, 1391–1418. [CrossRef]
40. Cheban, D.; Liu, Z. Periodic, quasi–periodic, almost periodic, almost automorphic, Birkhoff recurrent and Poisson stable solutions for stochastic differential equations. *J. Differ. Equ.* **2020**, *269*, 3652–3685. [CrossRef]
41. Alligood, K.; Sauer, T.; Yorke, J. *CHAOS: An Introduction to Dynamical Systems*; Springer: New York, NY, USA, 1996.
42. Devaney, R. *An Introduction to Chaotic Dynamical Systems*; Addison–Wesley: Menlo Park, CA, USA, 1990.
43. Skarda, C.; Freeman, W.J. How brains make chaos in order to make sense of the world? *Behav. Brain Sci.* **1987**, *10*, 161–173. [CrossRef]
44. Boccaletti, S.; Grebogi, C.; Lai, Y.; Mancini, H.; Maza, D. The control of chaos: Theory and applications. *Phys. Rep.* **2000**, *329*, 103–197. [CrossRef]
45. Wright, J. Simulation of EEG: Dynamic changes in synaptic efficacy, cerebral rhythms, and dissipative and generative activity in cortex. *Biol. Cybern.* **1999**, *81*, 131–147. [CrossRef]
46. Iasemidis, L.; Sackellares, J. REVIEW: Chaos Theory and Epilepsy. *Neuroscientist* **1996**, *2*, 118–126. [CrossRef]
47. Hoff, A. Chaos Control and Neural Classification. *Z. Naturforschung A* **1994**, *49*, 589–593. [CrossRef]
48. Hartman, P. *Ordinary Differential Equations*; Birkhauser: Boston, MA, USA, 2002.
49. Akhmet, M.; Fen, M. Poincare chaos and unpredictable functions. *Commun. Nonlinear Sci. Numer. Simul.* **2017**, *48*, 85–94. [CrossRef]

50. Zhang, H.; Lu, H.; Nayak, A. Periodic time series data analysis by deep learning methodology. *IEEE Access* **2020**, *8*, 078–088. [CrossRef]
51. Li, X.; Xu, F.; Zhang, J.; Wang, S. A multilayer feed forward small-world neural network controller and its application on electrohydraulic actuation system. *J. Appl. Math.* **2013**, *1*, 211–244. [CrossRef]
52. Wei, Y.; Zhang, Q. Square wave analysis. In *Common Waveform Analysis*; Cai, K.Y., Ed.; Springer: Boston, MA, USA, 2000; pp. 13–40.
53. Mohammad, U.; Yasin, M.; Yousuf, R.; Anwar, I. A novel square wave generator based on the translinear circuit scheme of second generation current controlled current conveyor–CCCII. *SN Appl. Sci.* **2019**, *1*, 587. [CrossRef]
54. Wu, U.; Yasin, M.; Yousuf, R.; Anwar, I. Deep convolutional neural network for structural dynamic response estimation and system identification. *J. Eng. Mech. Appl. Sci.* **2019**, *145*, 04018125. [CrossRef]